Fast Dynamic Programming for Elastic Registration of Curves

Javier Bernal[1]   Günay Doğan[1,2]   Charles R. Hagwood[1]

[1] National Institute of Standards and Technology,   [2] Theiss Research

{javier.bernal,gunay.dogan,charles.hagwood}@nist.gov

Abstract

Curve registration problems in data analysis and computer vision can often be reduced to the problem of matching two functions defined on an interval. Dynamic Programming (DP) is an effective approach to solve this problem. In this paper, we propose a DP algorithm that runs in $O(N)$ time to compute optimal diffeomorphisms for elastic registration of curves with N nodes. This algorithm contrasts favorably with other DP algorithms used for this problem: the commonly used algorithm of quadratic time complexity, and the algorithm that guarantees a globally optimal solution with $O(N^4)$ time complexity. Key to our computational efficiency is the savings achieved by reducing our search space, focusing on thin strips around graphs of estimates of optimal diffeomorphism. Estimates and strips are obtained with a multigrid approach: an optimal diffeomorphism obtained from a lower resolution grid using DP is progressively projected to ones of higher resolution until full resolution is attained. Additionally, our DP algorithm is designed so that it can handle nonuniformly discretized curves. This enables us to realize further savings in computations, since in the case of complicated curves requiring large numbers of nodes for a high-fidelity representation, we can distribute curve nodes adaptively, focusing nodes in parts of high variation. We demonstrate effectiveness of our DP algorithm on several registration problems in elastic shape analysis, and functional data analysis.

1. Introduction

Curve registration problems in data analysis and computer vision, e.g., horizontal alignment of chromatograms by domain warping, computation of elastic shape distances, can usually be reduced to the problem of matching two functions defined on an interval I in the real line. The problem of matching in turn usually involves computing an orientation-preserving diffeomorphism on the interval I to match each point in the range of one function with a point in the range of the other function, and vice versa. This is done by optimizing with respect to diffeomorphism, a data mis-match energy defined by data associated with the two functions. Dynamic Programming (DP) is widely recognized as an effective approach to solve such problems. However, although it computes globally optimal solutions, it is computationally expensive.

In the context of shape analysis, Srivastava et al. [1, 6, 9] proposed an algorithm for computing elastic shape distance between two closed curves in the plane using an $O(N^2)$ DP component for elastic registration of the curves, N the number of nodes per curve. It is computationally expensive as its total complexity is $O(N^3)$. A faster DP algorithm was proposed in [2] that works in a reduced search space (still $O(N^2)$ with a small constant), but computes very good diffeomorphisms. Note that a DP algorithm that would actually guarantee a globally optimal diffeomorphism by conducting a *complete* search would run in $O(N^4)$ time.

In what follows, we build on the works [5, 8], and describe computation in linear time of approximately optimal diffeomorphisms for elastic registration of curves. The diffeomorphisms are not guaranteed to be globally optimal, but we observed very convincing results in our experiments. Our DP approach uses concepts in [8], and similarly restricts its search to thin strips around graphs of estimates of optimal solution. It essentially uses a multigrid approach that projects, using DP, a diffeomorphism at a low resolution grid to one of higher resolution with this process continued recursively until a diffeomorphism of full resolution is obtained. This results in a fast $O(N)$ DP algorithm. We note, furthermore, that we implemented our DP to allow for curves of possibly unequal and nonuniform discretized domains of definition. In particular, our algorithm can be used for computing more efficiently elastic shape distances between closed curves in the plane with algorithms in [1, 9, 2, 3] by replacing their DP components with ours. We present numerical results showing that our algorithm is much faster than the aforementioned DP components, and that with it, in particular, shape distance computation in [9] is indeed much faster while still producing distances as good as before. Finally, we present numerical results from using our algorithm for alignment of chromatograms in context of elastic functional data analysis.

2. Elastic Registration Formulation

For $F : [0,1] \times [0,1] \times \mathbb{R} \to \mathbb{R}$, we minimize energies of the following general form with respect to γ, γ a diffeomorphism of $[0,1]$ onto itself with $\gamma(0) = 0, \gamma(1) = 1, \dot{\gamma} > 0$:

$$E(\gamma) = \int_0^1 F(t, \gamma(t), \dot{\gamma}(t))dt. \qquad (1)$$

Many problems we find in applications of computer vision and scientific data analysis fall in the category of nonlinear data fitting, in which a target data function $y : \mathbb{R} \to \mathbb{R}^d$ is given, and the problem is then that of fitting or registering a model $f : \mathbb{R} \times \mathbb{R} \to \mathbb{R}^d$ to this data. This problem is often solved by optimizing (1) above with respect to γ for $F(t, \gamma(t), \dot{\gamma}(t)) = \|y(t) - f(\gamma(t), \dot{\gamma}(t))\|^p$, $p \geqslant 1$, a nonlinear regression problem. The elastic curve registration problems that we address in this paper fall in this category.

In practice, we need to solve a discretized version of the problem, either because the data itself is discrete, or due to the need to approximate the functions numerically. Thus, given a positve integer N, we choose a partition (not necessarily uniform) $\{t_l\}_{l=1}^N$ of $[0,1]$, $t_1 = 0 < t_2 < \ldots < t_N = 1$, and discretize (1) with the trapezoidal rule:

$$E(\vec{\gamma}) = \frac{1}{2} \sum_{l=1}^{N-1} h_l(F(t_{l+1}, \gamma_{l+1}, \dot{\gamma}_{l+1}) + F(t_l, \gamma_l, \dot{\gamma}_l)),$$
$$(2)$$

where $\gamma_1 = 0, \gamma_N = 1$, $h_l = t_{l+1} - t_l$, $\gamma_l = \gamma(t_l)$, $\dot{\gamma}_l = (\gamma_{l+1} - \gamma_l)/h_l$, for $l = 1, \ldots, N-1$. We also add $\dot{\gamma}_N = \dot{\gamma}_1$ as a boundary condition for the derivative.

An important question then is the choice of discretization points $\{t_l\}_{l=1}^N$. This impacts both the efficiency and the
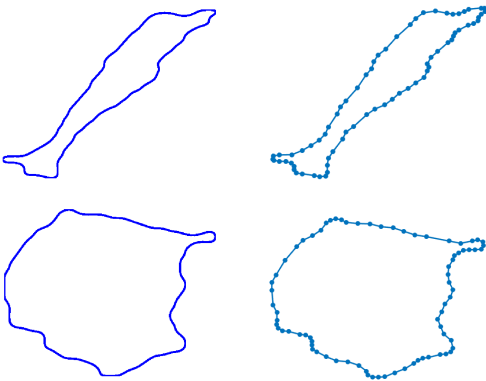

Figure 1. Adaptive nonuniform discretization of cell boundary curves. The curves on the left are high-fidelity uniformly sampled curves with $N = 1024$ nodes each. The curves on the right are adaptively sampled with $N = 74$ (top) and $N = 78$ (bottom) nodes, still maintaining a good representation of the geometry.

accuracy of the solution. We propose an adaptive nonuniform discretization scheme that follows the complexity of the input data. In the case of a curve $\beta(t) : [0,1] \to \mathbb{R}$ of curvature $\kappa(t)$, we can sample the curve to obtain nodes $\{\beta_l\}$, compute its discretized curvature $\{\kappa_l\}$ to measure geometric complexity, and choose discretization points accordingly. This motivates a two-step procedure

1. Distribute sample nodes $\{\beta_l\}$ such that pointwise geometric discretization error is below an acceptable tolerance: $\|\beta_l - \beta_{l-1}\|^2 \cdot \max(\kappa_l, \kappa_{l-1}) < 0.002$.

2. Compute lengths between consecutive nodes $\{\beta_l\}$, define arclength parameterization summing up lengths, and make discretization points associated with parametrization the choice of $\{t_l\}$.

Results of this procedure are illustrated in Figure 1.

3. Dynamic Programming (DP)

For positive integers N, M, not necessarily equal, and possibly nonuniform partitions of $[0,1]$, $\{t_i\}_{i=1}^N$, $t_1 = 0 < t_2 < \ldots < t_N = 1$, $\{z_j\}_{j=1}^M$, $z_1 = 0 < z_2 < \ldots < z_M = 1$, we consider the $N \times M$ grid on the unit square with grid points labeled (i,j), i, j integers, $1 \leq i \leq N, 1 \leq j \leq M$, each grid point (i,j) coinciding with planar point (t_i, z_j).

If the mesh of each partition, i.e., $\max(t_{m+1} - t_m), 1 \leq m \leq N-1$, and $\max(z_{m+1} - z_m), 1 \leq m \leq M-1$, is sufficiently small, then the set of diffeomorphisms γ of $[0,1]$ onto itself with $\gamma(0) = 0, \gamma(1) = 1, \dot{\gamma} > 0$, can be approximated by the set of homeomorphisms of $[0,1]$ onto itself whose graphs are piecewise linear paths from grid point $(1,1)$ to grid point (N,M) with grid points as vertices. We refer to the latter set as Γ. Then γ in Γ is an approximate diffeomorphism of $[0,1]$ onto itself and as such an energy conceptually faithful to (2) can be defined and computed for it. This is done one linear component of the graph of γ at a time.

Accordingly, given grid points (k,l), (i,j), $k < i, l < j$, that are endpoints of a linear component of the graph of γ, an energy of a trapezoidal nature over the line segment joining (k,l) and (i,j) is defined as follows:

$$E_{(k,l)}^{(i,j)} \equiv \frac{1}{2} \sum_{m=k}^{i-1} (t_{m+1} - t_m)(F_{m+1} + F_m), \qquad (3)$$

$$F_m \equiv F(t_m, \alpha(t_m), L)), m = k, \ldots, i.$$

Here α is the linear function from $[t_k, t_i]$ onto $[z_l, z_j]$ whose graph is the line segment, $\alpha(t_k) = z_l, \alpha(t_i) = z_j$, and L is the slope of the line segment. Note $L = \frac{z_j - z_l}{t_i - t_k} > 0$ as $z_j > z_l, t_i > t_k$. The energy for γ is then defined as the sum of the energies over the linear components of the graph of γ with α in (3) coinciding with γ on each component.

For the purpose of efficiently computing γ^* in Γ of minimum energy, we present algorithm in next section that uses DP on grid points in strips around graphs of estimates of γ^*, one strip at a time. In this algorithm, a general DP procedure, Procedure *DP*, whose outline follows, is executed, for each strip, on set R of grid points inside strip. For such sets computational cost is low (search space is relatively small), and their selection is such that it is highly likely final DP solution is γ^* itself or at least close to it. Since the collection of such strips has the appearance of one single strip whose shape evolves as it mimics the shapes of graphs of estimates of γ^*, we think of the collection as indeed being one single strip, a dynamic strip that we call *adapting* strip accordingly. In [2], Dogan, Bernal and Hagwood proposed using a strip R of linear ($O(N)$) width around the diagonal of $[0,1]^2$ connecting planar points $(0,0)$ and $(1,1)$, for a fast DP algorithm. In this work, rather than rigidly fixing R, we propose using an adapting strip as described above with a width that is constant ($O(1)$) as it evolves around graphs of estimates of γ^*. Obviously we do not know γ^*, but can estimate it using DP solutions on coarser grids. However, before going into the specifics of our proposed algorithm, we will describe Procedure *DP* operating on generic R.

The set R of labeled grid points can be any subset of the interior grid points plus the corner grid points $(1,1)$, (N,M). Given any such R, we denote by $\Gamma(R)$ the set of elements of Γ with all vertices in R. Accordingly, with the energy in (3) adjusted for R (see below), given positive integer $layrs$ (e.g., $layrs = 5$) which determines the size of certain neighborhoods to be searched (see below), then, based on DP, Procedure *DP* that follows, in $O(|R|)$ time, will often (depending on $layrs$) compute optimal γ^* in $\Gamma(R)$, $|R|$ the cardinality of R.

As the DP algorithm progresses over the indices (i,j) in R, it examines function values on indices (k,l) in a trailing neighborhood $N(i,j)$ of (i,j) (see Figure 2 for a particular R described below). In the full DP, we would be examining all (k,l) in R, $1 \leqslant k < i, 1 \leqslant l < j$. This has high computational cost, and is not necessary for our applications. Using a much smaller square neighborhood $N(i,j)$ of ω points ($\omega = layrs$) per side gives satisfactory results. Thus, for each (i,j) in R, we examine at most ω^2 indices (k,l) in the trailing neighborhood $N(i,j)$. Then the overall time complexity is $O(\omega^2|R|)$. We formally define $N(i,j)$ by

$$N(i,j) = \{(k,l) \in R : k \text{ is one of } \omega \text{ largest indices } < i$$
$$\text{and } l \text{ is one of } \omega \text{ largest indices } < j\}.$$

Note that in the unusual case $N(i,j)$ happens to be empty then a grid point (k,l) in R, $k < i$, $l < j$, perhaps $(k,l) = (1,1)$, is identified and $N(i,j)$ is set to $\{(k,l)\}$

The DP procedure follows. First, however, we clarify some implicit conventions in the procedure logic. The main loop in the DP procedure takes place over the single index i

(not the grid point (i,j)). We process index i in increasing order of its values, and for each value, each occurrence of the value is processed before moving to the next one. Also in the procedure, pairs of indices m_1, m_2 are retrieved from an index set $\mathcal{M}$, satisfying $m_1 < m_2$ with no other index in $\mathcal{M}$ greater than m_1 and less than m_2.

procedure *DP*
$\quad E(1,1) = 0$
$\quad$ **for** each $(i,j) \neq (1,1)$ in R in increasing order of i **do**
$\quad\quad$ **for** each $(k,l) \in N(i,j)$ **do**
$\quad\quad\quad \alpha = $ linear function, $\alpha(t_k) = z_l$, $\alpha(t_i) = z_j$
$\quad\quad\quad L = $ slope of line segment $\overline{(k,l)(i,j)}$
$\quad\quad\quad \mathcal{M} = \{m : k \leq m \leq i, \exists (m,n) \in R\}$
$\quad\quad\quad F_m = F(t_m, \alpha(t_m), L)$ for each $m \in \mathcal{M}$
$\quad\quad\quad E_{(k,l)}^{(i,j)} = \frac{1}{2} \sum_{m_1,m_2 \in \mathcal{M}} (t_{m_2} - t_{m_1})(F_{m_2} + F_{m_1})$
$\quad\quad$ **end for**
$\quad\quad E(i,j) = \min_{(k,l) \in N(i,j)} (E(k,l) + E_{(k,l)}^{(i,j)})$
$\quad\quad P(i,j) = \arg\min_{(k,l) \in N(i,j)} (E(k,l) + E_{(k,l)}^{(i,j)})$
$\quad$ **end for**
end procedure

The optimal solution γ^* in $\Gamma(R)$ can then be obtained by backtracking from (N,M) to $(1,1)$ with pointer P above. Accordingly, Procedure *opt-diffeom* that follows, will produce γ^* in the form $\vec{\gamma}^* = (\gamma_m^*)_{m=1}^N = (\gamma^*(t_m))_{m=1}^N$:

procedure *opt-diffeom*
$\quad \gamma_N^* = 1$
$\quad (i,j) = (N,M)$
$\quad$ **while** $(i,j) \neq (1,1)$ **do**
$\quad\quad (k,l) = P(i,j)$
$\quad\quad \gamma_k^* = z_l$
$\quad\quad$ **for** each integer m, $k < m < i$ **do**
$\quad\quad\quad \gamma_m^* = \frac{(t_i - t_m)}{(t_i - t_k)} z_l + \frac{(t_m - t_k)}{(t_i - t_k)} z_j$
$\quad\quad$ **end**
$\quad\quad (i,j) = (k,l)$
$\quad$ **end while**
end procedure

The original $O(N^2)$ DP algorithm, which we call *original-DP*, was used in [1, 6] to compute elastic shape distances. It is essentially the same as Procedure *DP* above (for the proper instance of (2)) followed by Procedure *opt-diffeom*, using a uniform grid, $N = M$, and R equal to all interior grid points plus the corner grid points $(1,1)$, (N,M). Depending on $layrs$, it computes optimal γ^* in Γ. In [2], a cheaper but still $O(N^2)$ version of *original-DP* called *fast-DP*, based on the Sakoe-Chiba Band [7], was presented for the same purpose. It is essentially *original-DP* with R equal to the corner grid points $(1,1)$, (N,M) plus interior grid points inside a strip S of width d along the diagonal of unit square from $(0,0)$ to $(1,1)$ (see Figure 2). Depending on $layers$ and d, it computes optimal γ^* in Γ.
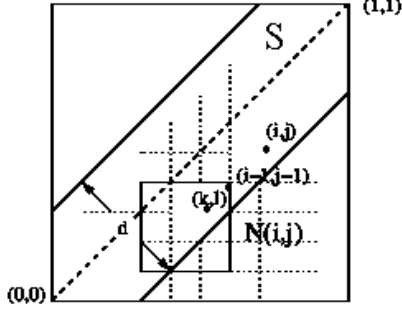
Figure 2. In *fast-DP*, R is set of interior grid points in strip S together with grid points at planar points $(0,0)$, $(1,1)$, i.e., $(1,1)$, (N, M). Given (i,j) in R, $i, j > 1$, then $N(i,j)$ in Procedure *DP* is the set of grid points in R on or inside the smaller square (here covering a 4×4 subgrid for $layrs = 4$) with right upper vertex $(i-1, j-1)$. Only the grid points in $N(i,j)$ are considered in Procedure *DP* for the left lower endpoint of line segment ending at (i,j) that makes $E(i,j)$ in Procedure *DP* the smallest.

4. Dynamic Programming Restricted to an Adapting Strip

The *DP* algorithms *original-DP* and *fast-DP* used in [1, 9, 2, 3] are essentially the same as Procedure *DP* (for the proper instance of (2)), using a uniform grid, $N = M$, and particular sets of grid points for R. Clearly, under these conditions, the possibility is then precluded of using either one of them for elastic registration of curves whose defining point sets have been either refined or coarsened due, for example, to curvature considerations.

In what follows, working with partitions (not necessarily uniform) of $[0,1]$, $\{t_l\}_{l=1}^N$, $\{z_l\}_{l=1}^M$, as previously described, we present a linear algorithm which we call *adapt-DP*, based on DP restricted to an adapting strip, to compute optimal diffeomorphisms for elastic registration of curves. It has parameters $layrs$, $lstrp$, set to small positive integers, say 5, 30, respectively. Parameter $layrs$ is as previously described, while $lstrp$ is an additional parameter that determines width of adapting strip (see below). Although *adapt-DP* is not guaranteed to be always successful, it has been observed to produce convincing results in our experiments. The original ideas for this algorithm are described in [5, 8] in the context of graph bisection and dynamic time warping.

As presented below, for a given instance of (2), *adapt-DP* is essentially an iterative process that restricts its search to the adapting strip around graphs of estimated solutions. Each iteration culminates with execution of Procedure *DP* for recursively projecting a diffeomorphism obtained from a lower resolution grid to one of higher resolution until full resolution is attained. For simplicity, we assume here $N = M = 2^n + 1$ for some positive integer n. Extension of the algorithm to allow N, M to have any values is straightforward. Note we don't assume partitions $\{t_l\}$, $\{z_l\}$

are uniform. Finally, after last execution of Procedure *DP* in *adapt-DP*, Procedure *opt-diffeom* is performed to obtain, depending on $layrs$ and $lstrp$, optimal γ^* in Γ. Algorithm *adapt-DP* follows:

algorithm *adapt-DP*
2. $I(1) = J(1) = 1$
3. $P(N, M) = (1, 1)$
   for $r = 1$ **to** n **do**
5. $NI = NJ = 2^r + 1$
6.   **for** $m = 1$ **to** $NI - 1$ **do**
7. $I(m+1) = m \cdot 2^{n-r} + 1$
8. $r'_m = \frac{1}{2}(t_{I(m)} + t_{I(m+1)})$
   end for
   for $m = 1$ **to** $NJ - 1$ **do**
     $J(m+1) = m \cdot 2^{n-r} + 1$
12. $s'_m = \frac{1}{2}(z_{J(m)} + z_{J(m+1)})$
   end for
14. $r'_1 = s'_1 = 0$
15. $r'_{NI-1} = s'_{NJ-1} = 1$
   $(i, j) = (N, M)$
   $D = \emptyset$
18.   **while** $(i, j) \neq (1, 1)$ **do**
     $(k, l) = P(i, j)$

****
20. Here below, for integers m', n', $1 < m' < NI$,
21. $1 < n' < NJ$, bin $B(m', n') \equiv$
22. $\{(x, y) : r'_{m'-1} \leq x \leq r'_{m'}, s'_{n'-1} \leq y \leq s'_{n'}\}$
****
     identify bins $B(m', n')$, $1 < m' < NI$,
     $1 < n' < NJ$, the interiors of which are
     intersected by line segment $\overline{(i,j)(k,l)}$
     $D' = \{(m', n') : \overline{(i,j)(k,l)} \cap B(m', n') \neq \emptyset\}$
     $D = D \cup D'$
     $(i, j) = (k, l)$
   end while
   $R = \{(1, 1), (N, M)\}$
31.   **for** each (m', n') in D **do**
     $i_0 = \max\{2, m' - lstrp\}$
     $j_0 = \max\{2, n' - lstrp\}$
     $R_1 = \{(i, j) : i = I(i'), i_0 \leq i' \leq m', j = J(n')\}$
     $R_2 = \{(i, j) : j = J(j'), j_0 \leq j' \leq n', i = I(m')\}$
     $R = R \cup R_1 \cup R_2$
   end for
38.   **execute** procedure *DP* on R
   end for
   execute procedure *opt-diffeom* to obtain γ^*
end algorithm

In outline of *adapt-DP* above, we note in line 5, NI starts equal to 3 (for $r = 1$) and then it is essentially doubled at each iteration $r > 1$ until it becomes equal to N at the nth iteration. We note in line 2 and in line 7 inside **for** loop at line 6, range of I starts with 3 integers (for $r = 1$)

and then essentially doubles in size at each iteration $r > 1$, contains previous range of I from preceding iteration, and is evenly spread in the set $\{1, 2, \ldots, N\}$ until it becomes this set. We note as well from the well-known sum of a geometric series that since $N = 2^n + 1$ then the sum of the NI's, i.e., $(2^1 + 1) + (2^2 + 1) + \ldots + (2^n + 1)$, is $O(N)$. Clearly, all of the above applies to NJ, M, and range of J.

We note **while** loop at line 18 identifies certain cells in the Voronoi diagram [11] of the set of grid points $R' \equiv \{(i, j) : i = I(m'), j = J(n'), 1 < m' < NI, 1 < n' < NJ\}$ restricted to the unit square. Indeed bin $B(m', n')$ as defined in lines 20-22, in terms of the computations in lines 8, 12, 14, 15, is exactly the Voronoi cell of $(I(m'), J(n'))$, and all such cells together partition the unit square. Accordingly, with γ^* encoded in P in line 3 ($r = 1$) or in line 38 ($r > 1$) through the execution of Procedure DP in the previous iteration ($r - 1$), it must be that every point in the graph of γ^* is in some bin $B(m', n')$. Thus, it then seems reasonable to say that a reliable region of influence of γ^* is the region around the graph of γ^* formed by the union of bins within a constant number of bins from the graph. Accordingly, to be precise, a bin B is part of this region if and only if there is a bin B', the interior of which the graph of γ^* intersects, B within a constant number ($lstrp$) of bins from B', B directly below or to the left of B', or B equal to B' (see Figure 3). We note that identifying this region is essentially accomplished in **while** loop at line 18 and **for** loop at line 31, with the region understood to be the union of bins or Voronoi cells $B(m', n')$ of grid points in R at the end of **for** loop. Clearly, the region contains the graph of γ^*, and has the appearance of a strip whose shape evolves from one iteration to the next as it closely mimics the shape of the graph of γ^* (see Figure 3), thus it is referred to as an adapting strip. Finally, we note that at the end of **for** loop, γ^* in $\Gamma(R) \subseteq \Gamma(R')$ encoded in P for current iteration is obtained in line 38 with Procedure DP restricted to the region or adapting strip, a region that as just described depends on all previous γ^* functions from previous iterations. The last γ^* obtained is then, depending on $layrs$, optimal in $\Gamma(R)$, and, depending on $layrs$ and $lstrp$, in $\Gamma(R')$.

With γ^* as above during the execution of **while** loop at line 18 for iteration r, we note that since γ^* is in $\Gamma(R)$ then the number of bins $B(m', n')$ whose interiors the graph of γ^* intersects must be $O(NI + NJ)$, which is also the time required to find them one linear component of the graph at a time. Since $|R|$ at end of **for** loop at line 31 is then $O(lstrp) \cdot O(NI + NJ)$, i.e., $O(NI + NJ)$, complexity of Procedure DP at line 38 is then $O(NI + NJ)$, and since as mentioned above the sum of the NI's and NJ's is $O(N)$ and $O(M)$, respectively, then the complexity of *adapt-DP* must be $O(N + M)$, implying *adapt-DP* is linear.
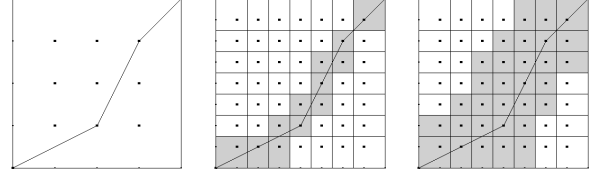

Figure 3. On left is γ^* from 2nd iteration, $NI = NJ = 2^2 + 1 = 5$. In center, during 3rd iteration, $NI = NJ = 2^3 + 1 = 9$; shaded bins are bins the interior of which γ^* intersects. On right, shaded bins form adapting strip in which next γ^* is computed. Each shaded bin is within 2 bins ($lstrp = 2$) from a bin whose interior current γ^* intersects, below or to the left of it or equal to it.

5. Applications and Experiments

In this section, we illustrate the effectiveness of Algorithm *adapt-DP* with several benchmarks and applications. We first compared it to *original-DP* [1, 9] and *fast-DP* [2] on synthetic applications. We examined both the computation times, and the accuracy of the solutions. Then we tested it on two important applications: elastic shape distances between 2d closed curves, and domain warping for alignment of functional data, specifically chromatograms. We report our findings in the respective subsections.

5.1. Synthetic Benchmarks

We evaluated *adapt-DP* using five synthetic curves in Figure 4 and γ functions shown in Figure 5. The γ functions were chosen to be difficult, having either small or steep gradients or both. We compared the results with those from *original-DP* and *fast-DP*. Given γ function, we reparametrized synthetic curve β_2 with it to obtain $\beta_1 = \beta_2(\gamma)$, and then with each algorithm tried to recover the discrete solution γ from the shape functions q_1, q_2 of β_1, β_2, respectively (see Subsection 5.2 for definition of shape functions), using $F(t, \gamma(t), \dot{\gamma}(t)) = \|q_1(t) - \sqrt{\dot{\gamma}(t)} q_2(\gamma(t))\|^2$ in (1). For various values of N (64, 128, 256, 512, 1024, 2048), and associated values of $layrs$ (64, 32, 16, 12, 12, 12, respectively), with $lstrp = 20$, we executed each algorithm, timed computations, and computed the L^2 error between the true solution γ^* and the computed γ, i.e., $\frac{1}{N-1}(\sum_{l=1}^{N-1} (\gamma(t_l) - \gamma^*(t_l))^2)^{\frac{1}{2}}$. Algorithm *adapt-DP* not only computed reasonable γ^* functions for all synthetic curves (L^2 errors were less than 10^{-3}), but was much faster than the other algorithms for $N \geq 256$ (see Figure 5 and Table 1).

5.2. Computation of Elastic Shape Distances

An elastic shape framework was introduced in [9] for finding geodesics in the shape space of closed curves and computing geodesic distances between elements of that space. Let closed curves $\beta_i : [0, 1] \rightarrow \mathbb{R}^2, i = 1, 2$ be of class C^2 and unit length. As each β_i is closed, it sat-
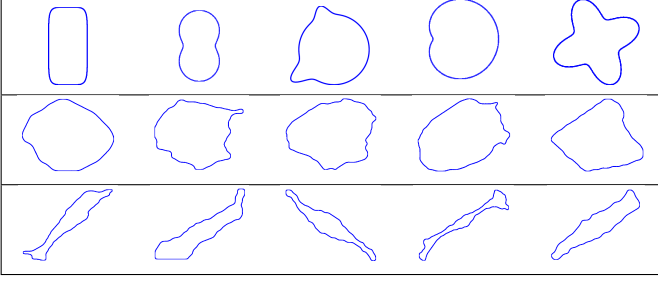
Figure 4. Curve examples used in the experiments. Synthetic curves: super ellipse, hippopede, bumps, limaçon, clover (top row); biological cell boundaries of type A and B (middle and bottom rows).
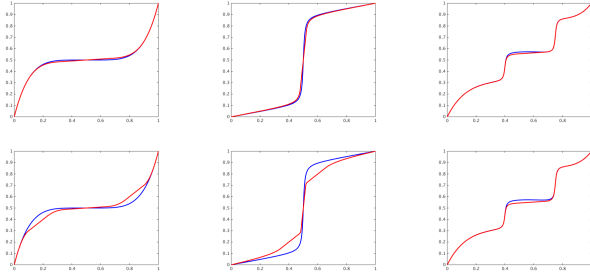

Figure 5. For γ^{flat} (left column in blue), *original-DP*, *fast-DP* with $d \approx 0.3\sqrt{2}$, and *adapt-DP* computed a reasonable γ^* (top left in red, L^2 error less than 10^{-3}), but *fast-DP* with $d \approx 0.2\sqrt{2}$ did not (bottom left, γ^* in red). The same can be said for γ^{steep} (middle column in blue). For γ^{bumpy} (right column in blue), *original-DP*, *fast-DP* with $d \approx 0.3\sqrt{2}$ and with $d \approx 0.2\sqrt{2}$ computed a reasonable γ^* (top right in red, L^2 error less than 10^{-3}). The same was true for *adapt-DP* which computed a slightly different γ^* (bottom right in red).

	$N =$	64	128	256	512	1024	2048
	$layrs =$	64	32	16	12	12	12
o-DP	all γ	0.49	1.26	1.00	2.07	8.48	34.3
f-DP	all γ	0.24	0.66	0.51	1.04	4.20	17.0
a-DP	γ^{flat}	0.65	0.67	0.27	0.29	0.57	1.20
	γ^{steep}	0.65	0.56	0.28	0.31	0.62	1.32
	γ^{bumpy}	0.81	1.04	0.37	0.36	0.70	1.46

Table 1. Times (in seconds) for limaçon with *original-DP* (*o-DP*), *fast-DP* (*f-DP*) with $d \approx 0.3\sqrt{2}$, and *adapt-DP* (*a-DP*). For *o-DP* and *f-DP*, the times depend only on N, not on γ, whereas for *a-DP*, the times depend on the shape of γ as well.

isfies $\beta_i(0) = \beta_i(1)$, $\dot{\beta}_i(0) = \dot{\beta}_i(1)$. We define $q_i(t) = \dot{\beta}_i(t)/\|\dot{\beta}_i(t)\|^{1/2}$ to be the shape function or square-root velocity function (SRVF) of β_i. Then the elastic shape distance between β_1 and β_2 is defined as the L^2 angle $\frac{\langle \hat{q}_1, \hat{q}_2 \rangle_{L^2}}{\|\hat{q}_1\|_{L^2}\|\hat{q}_2\|_{L^2}}$ between the optimally aligned SRVFs $\hat{q}_1$, $\hat{q}_2$,

$\hat{q}_1(t) = R(\theta)q_1(t + t_0)$, $\hat{q}_2(t) = \sqrt{\dot{\gamma}(t)}q_2(\gamma(t))$, where t_0 is the optimal seed or starting point, $R(\theta)$ is the 2×2 rotation matrix defined by the optimal rotation angle θ, and γ is the optimal reparameterization function (see [3]). The triple (t_0, θ, γ) for optimal alignment is then obtained by minimizing the mismatch energy:

$$E(t_0, \theta, \gamma) = \int_0^1 \|R(\theta)q_1(t + t_0) - \sqrt{\dot{\gamma}(t)}q_2(\gamma(t))\|^2 dt. \quad (4)$$

Note that, for fixed t_0, θ, (4) is in the same form as (1) for $F(t, \gamma(t), \dot{\gamma}(t)) = \|R(\theta)q_1(t+t_0) - \sqrt{\dot{\gamma}(t)}q_2(\gamma(t))\|^2$. We use the trapezoidal rule to write a discretized version of the mismatch energy (4),

$$E^h(t_0, \theta, \vec{\gamma}) = h \sum_{l=1}^{N-1} \|R(\theta)q_1(t_l + t_0) - \sqrt{\dot{\gamma}_l}q_2(\gamma_l)\|^2, \quad (5)$$

essentially adapting (2) to this particular case.

In practice, the curves β_i are available as discrete sets of curve nodes. In order to obtain the continuous SRVFs q_i needed in (5), we first compute discrete derivatives $\dot{\beta}_i$ with centered finite differences, and then compute the corresponding q_i, which we interpolate with cubic splines.

The minimization of (5) to obtain the optimal triple $(t_0, \theta, \vec{\gamma})$ is the most critical part of the shape distance computation. Although a *globally* optimal triple is required to compute the correct theoretical distance, a practical optimization algorithm to accomplish this goal is not available. Instead, various local optimization approaches have been proposed. The approach in [9] is to loop through the starting point t_0 candidates, to compute for each t_0 candidate the optimal rotation angle θ (assuming identity for initial $\vec{\gamma}$), and then to compute the optimal reparameterization $\vec{\gamma}$ for each fixed pair (t_0, θ) with DP, which is the most expensive step as it is $O(N^2)$ for each pair. This optimization scheme is a direct search algorithm with total time complexity of $O(N^3)$. Faster iterative algorithms were proposed in [4] and [2, 3]. In [4], Huang et al. used Riemannian optimization to achieve faster computation times and improved minimization results as compared to the direct search approach in [9]. In [2, 3], Dogan et al. proposed an alternating optimization algorithm that optimizes (t_0, θ) with FFT, and $\vec{\gamma}$ with an iterative solver based on constrained nonlinear optimization using the interior point method and initialized with fast-DP. They were able to demonstrate subquadratic running times in experiments. In this paper, we would like to demonstrate the efficiency gains from our new DP algorithm when used to compute elastic shape distances. For this purpose, we adopted the $O(N^3)$ algorithm in [9], and replaced its $O(N^2)$ *original-DP* step with our $O(N)$ *adapt-DP*. We were able to show improvement by an order of magnitude in computation times, while still computing shape distances as good as the original algorithm.

In order to examine scalability with respect to N, we computed with algorithm in [9] the shape distance between two synthetic curves, hippopede and bumps (see Figure 4), using *original-DP* and *adapt-DP*. Results are given in Table 2. The shape distances from both approaches agree very well. But we see that computation times with *original-DP* grow cubically, whereas with *adapt-DP* grow quadratically. For $N = 256, 512$ we then computed 10×10 pairwise shape distance matrices for cell boundary curves in Figure 4 as well, and observed the same efficiency gains. Algorithm in [9] with *adapt-DP* had total computation time that is a fraction of what it had with *original-DP*: 17 min, 1 hr by *adapt-DP* vs 50 min, 7 hrs by *original-DP* for $N = 256, 512$ respectively. A 5×5 submatrix of the distance matrix for $N = 512$ is shown in Table 3.

Additionally, we verified that *adapt-DP* indeed handles nonuniform discretizations correctly and produces results as good as the uniform case. For this, we took two cell boundary curves in Figure 4, β_1, the rightmost curve in middle row, and β_2, the rightmost curve in bottom row. We resampled them uniformly with equal numbers of nodes $N_1 = N_2 = 257$, and with $F(t, \gamma(t), \dot{\gamma}(t)) = \|q_1(t) - \sqrt{\dot{\gamma}(t)}q_2(\gamma(t))\|^2$ in (1), computed $\vec{\gamma}$ with *adapt-DP* for optimal matching, and $E(\vec{\gamma})$, the value of mismatch energy for $\vec{\gamma}$. We repeated this experiment for the nonuniform discretization of these curves obtained with the two-step procedure in Section 2. Optimal energy values and computation times are given below. Numerical results in the nonuniform case are as good as those of the uniform case at half the cost of computation time.

	N_1	N_2	$E(\vec{\gamma})$	time
Uniform	257	257	0.3786	0.291s
Nonuniform	163	149	0.3628	0.138s

5.3. Function Alignment by Warping

In the context of elastic functional data analysis, a framework was introduced in [10] for domain warping of functions in order to align them optimally by matching critical features, such as peaks.

For $i = 1, 2$, let $f_i : [0, 1] \to \mathbb{R}$ be functions in an appropriate space of functions (e.g., the space of absolutely continuous functions), and let $q_i : [0, 1] \to \mathbb{R}$ be the square-root slope function (SRSF) of f_i: $q_i(t) = \text{sign}(\dot{f}_i(t))\sqrt{|\dot{f}_i(t)|}$, $t \in [0, 1]$ (see [10]). Note the SRSF is the form the SRVF takes as f_i is real-valued.

As established in [10] the warping function γ that makes $f_2(\gamma)$ the optimal alignment of f_2 to f_1 is obtained by minimizing the following energy with respect to γ:

$$E(\gamma) = \int_0^1 (q_1(t) - \sqrt{\dot{\gamma}(t)}q_2(\gamma(t)))^2 dt, \qquad (6)$$

	Timings for $Dist(hippopede, bumps)$			
	$N = 64$	128	256	512
original-DP	0.50	3.53	28.7	227
adapt-DP	0.57	2.35	9.7	40
	Timings for $Dist(bumps, hippopede)$			
original-DP	0.56	3.74	30.2	228
adapt-DP	1.04	2.88	10.3	46
	Values for $Dist(hippopede, bumps)$			
original-DP	1.052	1.043	1.042	1.037
adapt-DP	1.048	1.040	1.042	1.037
	Values for $Dist(bumps, hippopede)$			
original-DP	1.128	1.114	1.101	1.091
adapt-DP	1.129	1.114	1.101	1.091

Table 2. The numerical values and running times (in seconds) for the elastic shape distance between the two synthetic curves: hippopede and bumps for increasing N.

.580/.580	.545/.542	.557/.555	.510/.507	.543/.541
.509/.508	.526/.524	.498/.496	.478/.478	.541/.539
.540/.540	.620/.619	.580/.580	.515/.513	.585/.585
.596/.596	.541/.540	.580/.579	.565/.564	.582/.580
.497/.496	.545/.544	.512/.509	.468/.467	.542/.541

Table 3. Matrix of pairwise shape distances of type A (rows) and type B (columns) cells. The first and second values of a pair computed using *original-DP* and *adapt-DP*, respectively.

where as before γ is a diffeomorphism of $[0, 1]$ onto itself with $\gamma(0) = 0, \gamma(1) = 1, \dot{\gamma}(t) > 0$. Note that (6) is in the same form as (1) for $F(t, \gamma(t), \dot{\gamma}(t)) = (q_1(t) - \sqrt{\dot{\gamma}(t)}q_2(\gamma(t)))^2$.

In [12] the alignment of chromatograms using the framework in [10] described above was demonstrated on liquid chromatography-mass spectrometry data for a chromatographically complex metabolomic reference sample. Computational results were presented in [12] from aligning two chromatograms in this manner. The chromatograms were taken in immediate succession under the conventional high performance liquid chromatography (HPLC) protocol described in [12]. As reported there, for chromatograms having 1,000 points, the aligning took 10 seconds on a desktop computer. In this work, we addressed much larger chromatograms (19,000+ points) for which *original-DP* was impractical. We aligned such chromatograms in a few minutes using *adapt-DP* with $lstrp = 150$ and $layrs = 12$ (see Figure 6). Timings for these experiments are given below:

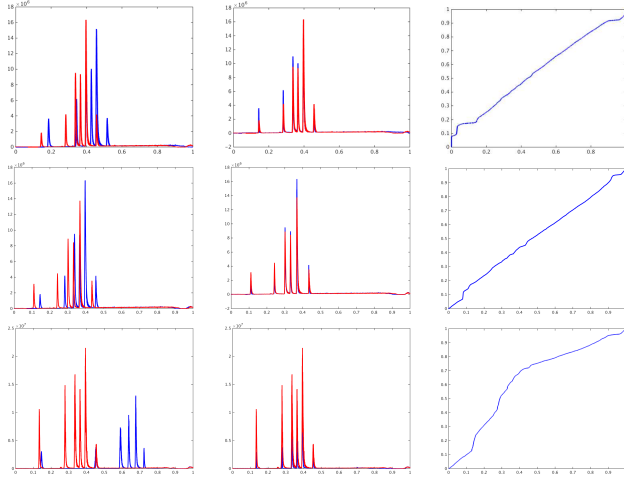|	Chromatogram 1	Chromatogram 2	time
Pair 1	19,713 pts	19,759 pts	180s
Pair 2	19,759 pts	26,474 pts	270s
Pair 3	19,693 pts	19,763 pts	172s

Figure 6. On left of each row, two chromatograms, one in blue and one in red of nonuniform time domains. In center, chromatograms in blue aligned to chromatograms in red after executions of *adapt-DP*. On right, plots of optimal piecewise warping functions.

6. Conclusions

In this paper, we propose a fast linear Dynamic Programming (DP) algorithm to compute optimal diffeomorphisms for elastic registration of curves. Although we cannot guarantee that it will always compute a globally optimal solution, we have observed very convincing results in our experiments. This algorithm which we call *adapt-DP* is based on ideas in [5, 8] in the context of graph bisection and dynamic time warping. We achieve considerable savings in computations and very favorable run times by restricting its search to thin strips around graphs of estimated solutions. It is essentially an iterative process that starts with a diffeomorphism computed at a very low resolution grid, projects at each iteration current diffeomorphism to one of double resolution using DP, and ends when a diffeomorphism of full resolution is obtained. This process runs with linear asymptotic time complexity with respect to the number of nodes on the given curves. We note, furthermore, *adapt-DP* has been implemented to allow for curves of possibly unequal and nonuniform discretized domains of definition. We use this flexibility to our advantage, to achieve further savings in computations, by not working with uniformly discretized curves, but with nonuniformly discretized curves of fewer nodes, as we concentrate nodes on parts with high curvature, and not so much on flat parts. We demonstrate the efficiency of *adapt-DP* with several examples. We achieve an order of magnitude gain in speed when we perform elastic shape analysis proposed in [9] with *adapt-DP*. We achieve even larger speed gains when we use *adapt-DP* for the alignment of chromatograms with large numbers of sample points. In particular, for chromatograms of 20,000 points,

we show this can be done in approximately 3 minutes.

A copy of adapt-DP with example data files and usage instructions can be obtained from the link: `http://math.nist.gov/˜JBernal` `/Fast_Dynamic_Programming.zip` We note that as currently implemented, *adapt-DP* uses only $F(t, \gamma(t), \dot{\gamma}(t)) = \|q_1(t) - \sqrt{\dot{\gamma}(t)}q_2(\gamma(t))\|^2$ in (1), $q_1, q_2 : [0,1] \to \mathbb{R}^d$, $d = 1$ or 2.

References

[1] Code from Statistical Shape Analysis and Modeling Group, Florida State University. http://ssamg.stat.fsu.edu/downloads/ClosedCurves2D3D.zip. Accessed: 2014-06-20.

[2] G. Doğan, J. Bernal, and C. Hagwood. A fast algorithm for elastic shape distances between closed planar curves. In *Proceedings of the IEEE Conference on Computer Vision and Pattern Recognition*, pages 4222–4230, June 2015.

[3] G. Doğan, J. Bernal, and C. Hagwood. FFT-based alignment of 2d closed curves with application to elastic shape analysis. In *Proceedings of the 1st International Workshop on Differential Geometry in Computer Vision for Analysis of Shape, Images and Trajectories (DIFF-CV) 2015, British Machine Vision Conference (BMVC)*, September 2015.

[4] W. Huang, K. A. Gallivan, A. Srivastava, and P.-A. Absil. Riemannian optimization for registration of curves in elastic shape analysis. *Journal of Mathematical Imaging and Vision*, 54(3):320–343, 2015.

[5] G. Karypis, R. Aggarwal, V. Kumar, and S. Shekhar. Multilevel hypergraph partitioning: Applications in VLSI domain. In *Proceedings of the Design and Automation Conference*, pages 526–530, 1997.

[6] W. Mio, A. Srivastava, and S. Joshi. On shape of plane elastic curves. *International Journal of Computer Vision*, 73(3):307–324, 2007.

[7] H. Sakoe and S. Chiba. Dynamic programming algorithm optimization for spoken word recognition. In *IEEE Trans. Acoustics, Speech, and Signal Proc.*, volume 26, 1978.

[8] S. Salvador and P. Chan. FastDTW: Toward accurate dynamic time warping in linear time and space. In *3rd Wkshp. on Mining Temporal and Sequential Data, ACM KDD '04*, August 2004.

[9] A. Srivastava, E. Klassen, S. Joshi, and I. Jermyn. Shape analysis of elastic curves in Euclidean spaces. *Pattern Analysis and Machine Intelligence, IEEE Transactions on*, 33(7):1415–1428, 2011.

[10] A. Srivastava, W. Wu, S. Kurtek, E. Klassen, and J. Marron. Statistical analysis and modeling of elastic functions. *ArXiv:1103.3817*, 2011.

[11] G. Voronoi. Nouvelles applications des paramètres continus à la théorie des formes quadratiques. *J. Reine Angew. Math.*, 133:97–178, 1908.

[12] W. E. Wallace, A. Srivastava, K. H. Telu, and Y. Simon-Manso. Pairwise alignment of chromatograms using an extended Fisher-Rao metric. *Analytica Chimica Acta 841*, pages 10–16, 2014.